



# High sensing properties of Ce-doped $\alpha$ -Fe<sub>2</sub>O<sub>3</sub> nanotubes to acetone

Changbai Liu<sup>a</sup>, Hao Shan<sup>b</sup>, Li Liu<sup>b,\*</sup>, Shouchun Li<sup>b</sup>, Haiying Li<sup>b</sup>

<sup>a</sup>College of Electronic Science & Engineering, Jilin University, Changchun 130012, PR China

<sup>b</sup>State Key Laboratory of Superhard Materials, College of Physics, Jilin University, Changchun 130012, PR China

Received 29 June 2013; received in revised form 2 August 2013; accepted 2 August 2013

Available online 11 August 2013

## Abstract

Pristine and Ce-doped (3, 4, 5 at% Ce)  $\alpha$ -Fe<sub>2</sub>O<sub>3</sub> nanotubes were synthesized by electrospinning method. The morphologies and structures of these samples were characterized by scanning electron microscope (SEM) and X-ray powder diffraction (XRD). The gas sensing properties of the four samples were investigated. The results showed that the sensitivity of the 4 at% Ce-doped  $\alpha$ -Fe<sub>2</sub>O<sub>3</sub> nanotubes reached 21.5–50 ppm acetone at 240 °C, which was about 8.3 times larger than that of pure  $\alpha$ -Fe<sub>2</sub>O<sub>3</sub> nanotubes. Meantime, the response and recovery times were about 3 and 8 s, respectively. The sensitivity of the lowest detecting limit to 1 ppm acetone was about 3. Moreover, the sensor also possessed the good selectivity and long-term stability to acetone.

© 2013 Elsevier Ltd and Techna Group S.r.l. All rights reserved.

**Keywords:** Acetone;  $\alpha$ -Fe<sub>2</sub>O<sub>3</sub>; Ce; Gas sensor; Nanotubes

## 1. Introduction

Semiconductors oxides have attracted considerable attention around the world, because of their multitudinous applications in photosensitization [1], photocatalysis [2], magnetism [3], batteries [4] and gas sensors [5]. Nowadays, due to an urgent necessary in air-quality detection and environmental monitoring, the application field of semiconductors oxides in gas sensors has been more and more important. Owing to the low cost and easy availability, various semiconductors oxides, just like ZnO, SnO<sub>2</sub>, Fe<sub>2</sub>O<sub>3</sub>, WO<sub>3</sub>, In<sub>2</sub>O<sub>3</sub>, TiO<sub>2</sub>, have been used to act as the gas sensitive materials to detect ethanol, acetone, toluene, H<sub>2</sub>, CO, H<sub>2</sub>S, formaldehyde [6–13]. However, as the high requirements of detection precision of pollution gases, the shortcomings of these semiconductors oxides come out gradually, such as high operating temperature, low sensitivity, poor selectivity and bad stability. Cerium, a kind of lanthanide elements, has been proved to be an effective dopant element to enhance the gas sensing properties of semiconductors oxides. For instance, Song et al. have proved that Ce doped SnO<sub>2</sub> exhibited a higher sensitive toward acetone than pure SnO<sub>2</sub>

[14]. Mohammadi et al. have demonstrated that Ce doped TiO<sub>2</sub> gas sensors have a good capability for the detection of low concentration of CO [15]. Luo et al. have reported that the sensitivity of WO<sub>3</sub> to xylene is enhanced significantly after doping with Ce [16]. However, the gas sensing properties of Ce doped  $\alpha$ -Fe<sub>2</sub>O<sub>3</sub> have rarely been reported.

$\alpha$ -Fe<sub>2</sub>O<sub>3</sub> is a common and potential n-type semiconductor, which has been widely applied in pigment [17], catalysts [18], batteries [19], gas sensors [6] and drug delivery [20]. Especially,  $\alpha$ -Fe<sub>2</sub>O<sub>3</sub> nanotubes have been more and more important in the field of gas sensors in recent years, due to its hollow structure and large specific surface area. In this paper, we synthesize Ce doped  $\alpha$ -Fe<sub>2</sub>O<sub>3</sub> nanotubes and investigate their gas sensing properties. The results show that the as-prepared Ce doped  $\alpha$ -Fe<sub>2</sub>O<sub>3</sub> nanotubes possess an excellent sensitivity to acetone.

## 2. Experimental procedure

All the chemical reagents used were analytical grade and used without further purification. Fe(NO<sub>3</sub>)<sub>3</sub> · 6H<sub>2</sub>O, Ce(NO<sub>3</sub>)<sub>3</sub> · 6H<sub>2</sub>O, N,N-dimethylformamide (DMF) and ethanol were obtained

\*Corresponding author. Tel./fax: +86 431 850 2260.

E-mail addresses: [liul99@jlu.edu.cn](mailto:liul99@jlu.edu.cn), [liuli\\_teacher@163.com](mailto:liuli_teacher@163.com) (L. Liu).

from Aladdin (China). Poly(vinyl pyrrolidone) (PVP, Mw=1,300,000) was purchased from Sigma-Aldrich (USA).

The procedure of electrospinning was according to the reported paper [5]. Typically, 0.7 g  $\text{Fe}(\text{NO}_3)_3 \cdot 6\text{H}_2\text{O}$  was dissolved with the 1:1 weight ratio of DMF and ethanol under vigorous magnetic stirring for 30 min. After that, 0.5 g PVP was added and kept stirring to form a clear and homogenous solution. At last,  $\text{Ce}(\text{NO}_3)_3 \cdot 6\text{H}_2\text{O}$  was added in a ratio of Ce/Fe=0 at%, 3 at%, 4 at%, 5 at%. After stirred for 12 h, the mixture solution was loaded into a syringe and ejected under the voltage of 15 kV and the distance of 20 cm between the anode and cathode. The electrospun composite fibers were calcinated at 500 °C for 4 h. Finally, the pure and Ce doped  $\alpha\text{-Fe}_2\text{O}_3$  nanotubes were obtained.

Structure analysis with X-ray diffraction (XRD) was conducted on a PANalytical B.V. Empyrean X-ray diffractometer with Cu  $K\alpha$  radiation ( $\lambda=1.5418 \text{ \AA}$ ). Scanning electron microscope (SEM) images were performed on a FEI XL30 instrument.

The process of gas sensors fabrication and the gas sensing properties tests have been described in our previous work [8]. The sample was mixed with deionized water to form a paste. The paste was coated on a ceramic tube on which a pair of gold electrodes was previously printed, and then a Ni–Cr heating wire was inserted in the tube to form a gas sensor. The thickness of the sensing film was measured to be about 300  $\mu\text{m}$ . The gas sensor was dried and aged for 10 days before the first measurement. Gas sensing properties were measured by a CGS-8 intelligent gas sensing analysis system (Beijing Elite Tech Co., Ltd., China). The testing ambience was controlled by a DGD-III dynamic gas distribution system. The background gas was artificial air. Gas sensor was inserted in the sensor sockets in the test chamber (1 L in volume).

When the resistance of sensor was stable, target gas was introduced into the chamber through a steel plug. After the sensor resistance reached a new constant value, the position of the sensor was turned so that the sensor could be surrounded by air quickly. The sensing tests were performed in a super-clean room with a constant temperature of 25 °C. In our paper, the sensor response was defined as  $S=R_a/R_g$ , where  $R_a$  is the resistance in ambient air and  $R_g$  is the resistance in tested gas, respectively. The response and recovery time were defined as the time taken by the sensor to achieve 90% of the total resistance change in the case of adsorption and desorption, respectively.

### 3. Results and discussion

The structures and morphologies of all samples are characterized by SEM, and the results are shown in Fig. 1. We can see from Fig. 1 that, these nanofibers are distributed disorderly and unsystematic. The structure of nanotubes can be clearly indicated from the four insets. Compared with the pure  $\alpha\text{-Fe}_2\text{O}_3$ , the surfaces of nanotubes of Ce-doped (3, 4, 5 at%)  $\alpha\text{-Fe}_2\text{O}_3$  are more coarser, which can be benefit the gas absorption.

Fig. 2 shows the XRD patterns of pristine and Ce-doped (3, 4, and 5 at%)  $\alpha\text{-Fe}_2\text{O}_3$  nanotubes. The main peaks can be indexed as cubic single crystal  $\text{Fe}_2\text{O}_3$ , with lattice constants of  $a=c=8.351 \text{ \AA}$ . These parameters agree well with the reported values from the JCPDS card (39-1346).

The sensitivities of gas sensors based on pristine and Ce-doped (3, 4, and 5 at%)  $\alpha\text{-Fe}_2\text{O}_3$  nanotubes to 50 ppm acetone were measured at different temperatures in order to find the optimal working temperature. The results are shown in Fig. 3. The responses of the four samples increase with the rising of

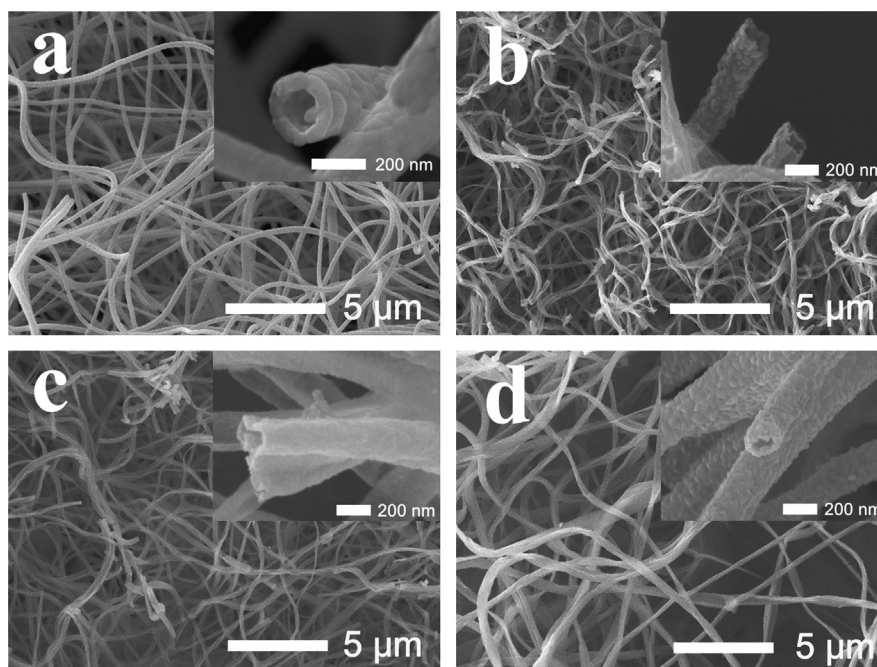


Fig. 1. SEM images of (a) pure, (b) 3 at%, (c) 4 at%, (d) 5 at% Ce-doped  $\alpha\text{-Fe}_2\text{O}_3$  nanotubes.

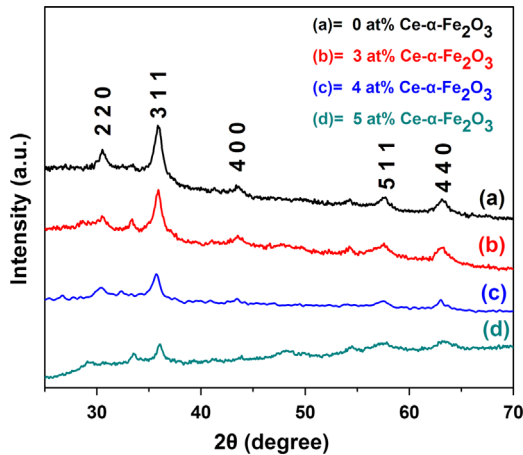


Fig. 2. XRD patterns of pristine and Ce-doped (3, 4, and 5 at%)  $\alpha$ -Fe<sub>2</sub>O<sub>3</sub> nanotubes.

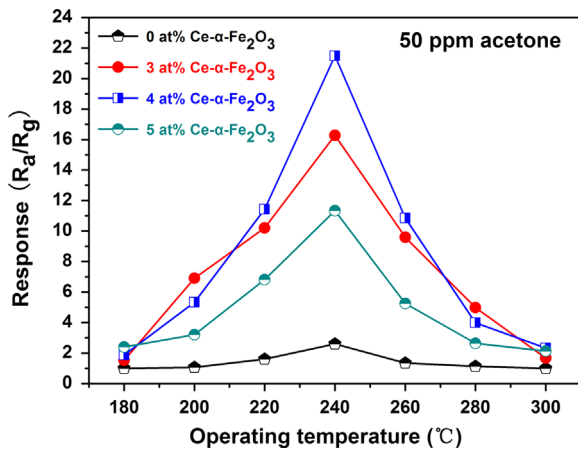


Fig. 3. Responses of gas sensors based on pristine and Ce-doped (3, 4, and 5 at%)  $\alpha$ -Fe<sub>2</sub>O<sub>3</sub> nanotubes to 50 ppm acetone under different temperatures.

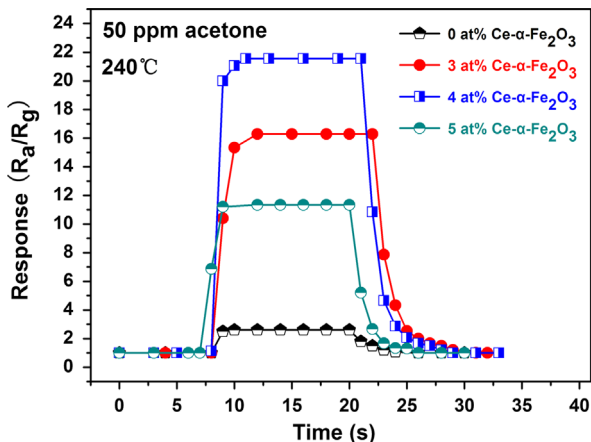


Fig. 4. Response and recovery curves of gas sensors based on pristine and Ce-doped (3, 4, and 5 at%)  $\alpha$ -Fe<sub>2</sub>O<sub>3</sub> nanotubes to 50 ppm acetone at 240 °C.

the operating temperature, and reach their maximum at 240 °C. Then, as the operating temperature continue to increase, the responses decrease. The sensitivity of gas sensor based on 4 at

Table 1

Response and recovery times of pristine and Ce-doped (3, 4, and 5 at% Ce)  $\alpha$ -Fe<sub>2</sub>O<sub>3</sub> nanotubes sensors.

Sample	Response time (s)	Recovery time (s)
pure $\alpha$ -Fe <sub>2</sub> O <sub>3</sub> nanotubes	2	4
3 at% Ce-doped $\alpha$ -Fe <sub>2</sub> O <sub>3</sub> nanotubes	4	8
4 at% Ce-doped $\alpha$ -Fe <sub>2</sub> O <sub>3</sub> nanotubes	3	8
5 at% Ce-doped $\alpha$ -Fe <sub>2</sub> O <sub>3</sub> nanotubes	5	6

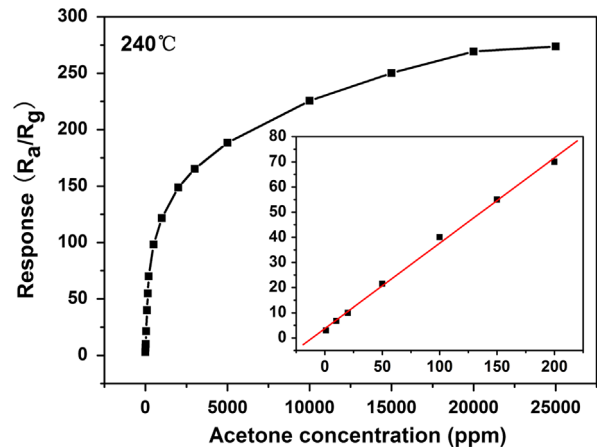


Fig. 5. Responses of 4 at% Ce-doped  $\alpha$ -Fe<sub>2</sub>O<sub>3</sub> nanotubes to different concentrations of acetone at 240 °C; the inset shows the linear line of the response in the acetone concentration of 1–200 ppm.

% Ce-doped  $\alpha$ -Fe<sub>2</sub>O<sub>3</sub> nanotubes to 50 ppm acetone is 21.5, which is about 8.3 times larger than that of the gas sensor based on the pure  $\alpha$ -Fe<sub>2</sub>O<sub>3</sub> nanotubes, indicating that the doping of Ce can enhance the sensitivity of  $\alpha$ -Fe<sub>2</sub>O<sub>3</sub> nanotubes significantly.

The response and recovery characteristic is one of the important features of gas sensors. The response and recovery curves of gas sensors based on pristine and Ce-doped (3, 4, 5 at%)  $\alpha$ -Fe<sub>2</sub>O<sub>3</sub> nanotubes to 50 ppm acetone at 240 °C are shown in Fig. 4. From the figure we can see that, although Ce doping in different amount, the response and recovery times of each sample change slightly. The response and recovery times of all samples can be seen in Table 1.

Fig. 5 shows the responses of 4 at% Ce-doped  $\alpha$ -Fe<sub>2</sub>O<sub>3</sub> nanotubes to different concentrations of acetone at 240 °C. The inset of Fig. 5 shows the linear line of the response in the acetone concentration of 1–200 ppm. From the figure we can see that, the response increases rapidly with the increasing of the acetone concentration in the range of 1–5000 ppm. Then, the response rises slowly and finally reaches saturation at about 25,000 ppm. The lowest detecting limit of the gas sensor based on 4 at% Ce-doped  $\alpha$ -Fe<sub>2</sub>O<sub>3</sub> nanotubes can reach 1 ppm, and the value is about 3.

The selectivity of gas sensor based on 4 at% Ce-doped  $\alpha$ -Fe<sub>2</sub>O<sub>3</sub> nanotubes was measured by exposed the sensor to 10, 50 and 200 ppm acetone, formaldehyde, toluene, ammonia, hydrogen, carbon monoxide and butane at 240 °C. The results are shown in Fig. 6. It is clearly to point out that the sensor is

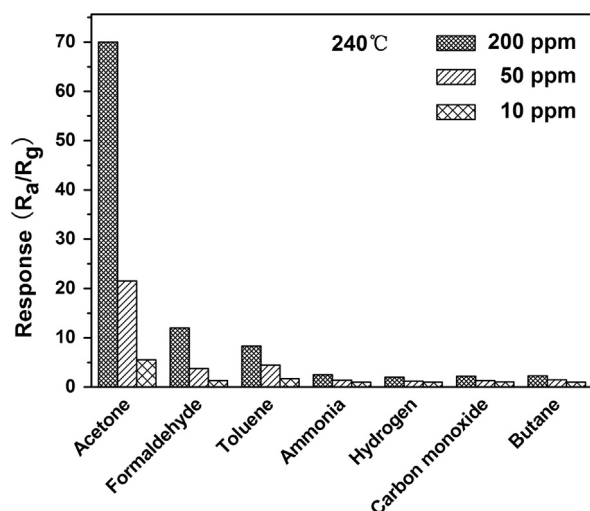


Fig. 6. Responses of gas sensor based on 4 at% Ce-doped  $\alpha$ -Fe<sub>2</sub>O<sub>3</sub> nanotubes to 10, 50 and 200 ppm acetone, formaldehyde, toluene, ammonia, hydrogen, carbon monoxide and butane at 240 °C.

less sensitive to formaldehyde and toluene, and almost insensitive to ammonia, hydrogen, carbon monoxide and butane. The results demonstrate the good selectivity of gas sensor based on 4 at% Ce-doped  $\alpha$ -Fe<sub>2</sub>O<sub>3</sub> nanotubes.

The long-term stability of gas sensor based on 4 at% Ce-doped  $\alpha$ -Fe<sub>2</sub>O<sub>3</sub> nanotubes to acetone has been also measured at 240 °C and shown in Fig. 7. It can be seen that the sensors exhibit nearly constant sensor signals to 10, 50, 100 and 200 ppm acetone during the tests, confirming the good stability of the sensor.

The mechanism of gas sensing can be explained by the gas adsorption and the chemical reactions on the surface of the materials [21]. When  $\alpha$ -Fe<sub>2</sub>O<sub>3</sub> nanotubes are exposed to the air, their surface will be surrounded by oxygen molecules. These oxygen molecules will extract electrons from the conduction band of the  $\alpha$ -Fe<sub>2</sub>O<sub>3</sub> and ionize to O<sup>2-</sup>, O<sup>-</sup>, O<sub>2</sub><sup>-</sup>. This will lead to conductivity decreasing of  $\alpha$ -Fe<sub>2</sub>O<sub>3</sub>. However, when  $\alpha$ -Fe<sub>2</sub>O<sub>3</sub> nanotubes are exposed to acetone, the surrounding acetone molecules will react with these ionized oxygen species and release the trapped electrons back to the  $\alpha$ -Fe<sub>2</sub>O<sub>3</sub>. Thus increase the conductivity of  $\alpha$ -Fe<sub>2</sub>O<sub>3</sub>.

Moreover, the structure of nanotubes can also help to improve the sensitivity of  $\alpha$ -Fe<sub>2</sub>O<sub>3</sub> to acetone. At first, the hollow structure of nanotubes can facilitate the oxygen and acetone molecules transportation, which will accelerate the process of reactions [22]. Then, the characteristic of large specific surface area of nanotubes can adsorb more oxygen molecules and offer more reaction sites for them [23]. These two advantages result to an enhanced sensitivity.

Compared with the pure  $\alpha$ -Fe<sub>2</sub>O<sub>3</sub> nanotubes, the sensitivity of Ce doped  $\alpha$ -Fe<sub>2</sub>O<sub>3</sub> nanotubes has been increased remarkably. Two reasons can be used to explain the phenomenon. Firstly, the surface of  $\alpha$ -Fe<sub>2</sub>O<sub>3</sub> nanotubes will form more defects after doping Ce<sup>4+</sup>. The coarser surfaces can result to a large contact area between the material and the gas, which will convenient to adsorbed more oxygen molecules [14]. Secondly, Ce can act as a catalyst, which can support the catalytic

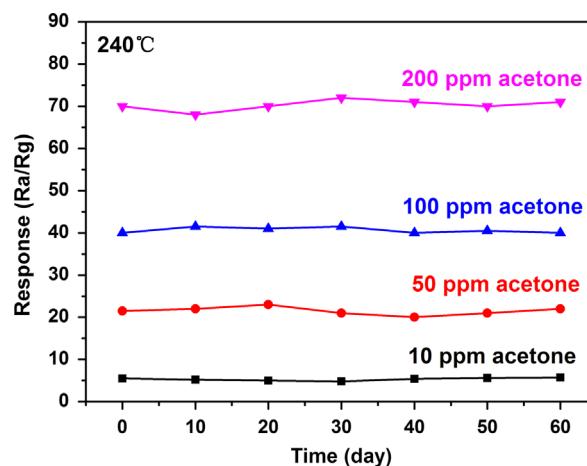


Fig. 7. Long-term stability of gas sensor based on 4 at% Ce-doped  $\alpha$ -Fe<sub>2</sub>O<sub>3</sub> nanotubes to 10, 50, 100 and 200 ppm acetone at 240 °C.

conversion of the reducing gas into the respective oxidation product [24]. However, more amount of Ce doping results to a low sensitivity, which may be due to superfluous Ce can decrease the effective reaction areas between gas sensitive materials and target gas.

#### 4. Conclusion

In summary, pristine and Ce-doped (3, 4, 5 at% Ce)  $\alpha$ -Fe<sub>2</sub>O<sub>3</sub> nanotubes are synthesized by electrospinning method and their gas sensing properties are investigated. The sensitivity, recovery time and response time of this sample (4 at% Ce) towards 50 ppm at 240 °C were 21.5, 3 s and 8 s, respectively. The lowest detecting limit of the sensor can reach 1 ppm. The sensitivity of the pure  $\alpha$ -Fe<sub>2</sub>O<sub>3</sub> nanotubes gas sensor has been improved by more than 8 times after doping with 4 at% Ce. Moreover, the sensor (4 at% Ce) also shows good selectivity and long-term stability to acetone.

#### Acknowledgments

The work has been supported by the Jilin Environment Office (2009-22), Jilin Provincial Science and Technology Department (20100344), and the National Innovation Experiment Program for University Students (2010C65188).

#### References

- [1] K.S. Leschkes, R. Divakar, J. Basu, E. Enache-Pommer, J.E. Boercker, C.B. Carter, U.R. Kortshagen, D.J. Norris, E.S. Aydil, Photosensitization of ZnO nanowires with CdSe quantum dots for photovoltaic devices, *Nano Letters* 7 (2007) 1793–1798.
- [2] A. Fujishima, X.T. Zhang, D.A. Tryk, TiO<sub>2</sub> photocatalysis and related surface phenomena, *Surface Science Reports* 63 (2008) 515–582.
- [3] D. Jagadeesan, U. Mansoori, P. Mandal, A. Sundaresan, M. Eswaramoorthy, Hollow Spheres to Nanocups: tuning the Morphology and Magnetic Properties of Single-Crystalline  $\alpha$ -Fe<sub>2</sub>O<sub>3</sub> Nanostructures, *Angewandte Chemie International Edition* 120 (2008) 7799–7802.
- [4] A. Brandt, A. Balducci, Ferrocene as precursor for carbon-coated alpha-Fe<sub>2</sub>O<sub>3</sub> nano-particles for rechargeable lithium batteries, *Journal of Power Sources* 230 (2013) 44–49.

- [5] L. Liu, Z. Zhong, Z. Wang, L. Wang, S. Li, Z. Liu, Y. Han, Y. Tian, P. Wu, X. Meng, Synthesis, characterization, and m-xylene sensing properties of Co-ZnO composite nanofibers, *Journal of the American Ceramic Society* 94 (2011) 3437–3441.
- [6] W. Zheng, Z. Li, H. Zhang, W. Wang, Y. Wang, C. Wang, Electrospinning route for  $\alpha$ -Fe<sub>2</sub>O<sub>3</sub> ceramic nanofibers and their gas sensing properties, *Materials Research Bulletin* 44 (2009) 1432–1436.
- [7] P. Song, Q. Wang, Z. Yang, Acetone sensing characteristics of ZnO hollow spheres prepared by one-pot hydrothermal reaction, *Materials Letters* 86 (2012) 168–170.
- [8] L. Liu, C. Liu, S. Li, L. Wang, H. Shan, X. Zhang, H. Guan, Z. Liu, Honeycombed SnO<sub>2</sub> with ultra sensitive properties to H<sub>2</sub>, *Sensors and Actuators B* 177 (2013) 893–897.
- [9] S.K. Lim, S.H. Hwang, D. Chang, S. Kim, Preparation of mesoporous In<sub>2</sub>O<sub>3</sub> nanofibers by electrospinning and their application as a CO gas sensor, *Sensors and Actuators B* 149 (2010) 28–33.
- [10] Z. Wen, L. Tian-mo, L. De-jun, Formaldehyde gas sensing property and mechanism of TiO<sub>2</sub>-Ag nanocomposite, *Physica B* 405 (2010) 4235–4239.
- [11] J.M. Ma, L. Mei, Y.J. Chen, Q.H. Li, T.H. Wang, Z. Xu, X.C. Duan, W.J. Zheng, alpha-Fe<sub>2</sub>O<sub>3</sub> nanochains: ammonium acetate-based ionothermal synthesis and ultrasensitive sensors for low-ppm-level H<sub>2</sub>S gas, *Nanoscale* 5 (2013) 895–898.
- [12] Q. Qi, T. Zhang, L. Liu, X. Zheng, Synthesis and toluene sensing properties of SnO<sub>2</sub> nanofibers, *Sensors and Actuators B* 137 (2009) 471–475.
- [13] M. Zhao, J.X. Huang, C.W. Ong, Room-temperature resistive H<sub>2</sub> sensing response of Pd/WO<sub>3</sub> nanocluster-based highly porous film, *Nanotechnology* 23 (2012) 315503.
- [14] P. Song, Q. Wang, Z. Yang, Preparation, characterization and acetone sensing properties of Ce-doped SnO<sub>2</sub> hollow spheres, *Sensors and Actuators B* 173 (2012) 839–846.
- [15] M.R. Mohammadi, D.J. Fray, Nanostructured TiO<sub>2</sub>-CeO<sub>2</sub> mixed oxides by an aqueous sol-gel process: effect of Ce:Ti molar ratio on physical and sensing properties, *Sensors and Actuators B* 150 (2010) 631–640.
- [16] S. Luo, G. Fu, H. Chen, Z. Liu, Q. Hong, Gas-sensing properties and complex impedance analysis of Ce-added WO<sub>3</sub> nanoparticles to VOC gases, *Solid-State Electronics* 51 (2007) 913–919.
- [17] M. Llusar, V. Royo, J. Badenes, M. Tena, G. Monrós, Nanocomposite Fe<sub>2</sub>O<sub>3</sub>-SiO<sub>2</sub> inclusion pigments from post-functionalized mesoporous silicas, *Journal of the European Ceramic Society* 29 (2009) 3319–3332.
- [18] Z. Zhong, J. Ho, J. Teo, S. Shen, A. Gedanken, Synthesis of porous  $\alpha$ -Fe<sub>2</sub>O<sub>3</sub> nanorods and deposition of very small gold particles in the pores for catalytic oxidation of CO, *Chemistry of Materials* 19 (2007) 4776–4782.
- [19] Z. Wang, D. Luan, S. Madhavi, C.M. Li, X.W. Lou,  $\alpha$ -Fe<sub>2</sub>O<sub>3</sub> nanotubes with superior lithium storage capability, *Chemical Communications* 47 (2011) 8061.
- [20] P.C. Wu, W.S. Wang, Y.T. Huang, H.S. Sheu, Y.W. Lo, T.L. Tsai, D.B. Shieh, C.S. Yeh, Porous iron oxide based nanorods developed as delivery nanocapsules, *Chemistry – A European Journal* 13 (2007) 3878–3885.
- [21] J. Ma, J. Teo, L. Mei, Z. Zhong, Q. Li, T. Wang, X. Duan, J. Lian, W. Zheng, Porous platelike hematite mesocrystals: synthesis, catalytic and gas-sensing applications, *Journal of Materials Chemistry* 22 (2012) 11694.
- [22] X. Chen, Z. Guo, W.H. Xu, H.B. Yao, M.Q. Li, J.H. Liu, X.J. Huang, S.H. Yu, Templating Synthesis of SnO<sub>2</sub> Nanotubes Loaded with Ag<sub>2</sub>O Nanoparticles and Their Enhanced Gas Sensing Properties, *Advanced Functional Materials* 21 (2011) 2049–2056.
- [23] N. Du, H. Zhang, B. Chen, X. Ma, Z. Liu, J. Wu, D. Yang, Porous Indium Oxide Nanotubes: layer-by-Layer Assembly on Carbon-Nanotube Templates and Application for Room-Temperature NH<sub>3</sub> Gas Sensors, *Advanced Materials* 19 (2007) 1641–1645.
- [24] D. Liu, T. Liu, H. Zhang, C. Lv, W. Zeng, J. Zhang, Gas sensing mechanism and properties of Ce-doped SnO<sub>2</sub> sensors for volatile organic compounds, *Materials Science in Semiconductor Processing* 15 (2012) 438–444.